ACES Asian Chemical Editorial Society
DOI: 10.1002/cnma.201700055
CHEMNANOMAT
Focus Review

Energy-Storage Materials

SPECIAL ISSUE

Graphene/Polymer Nanocomposites for Supercapacitors

Xiaoyan Zhang and Paolo Samorì*[a]

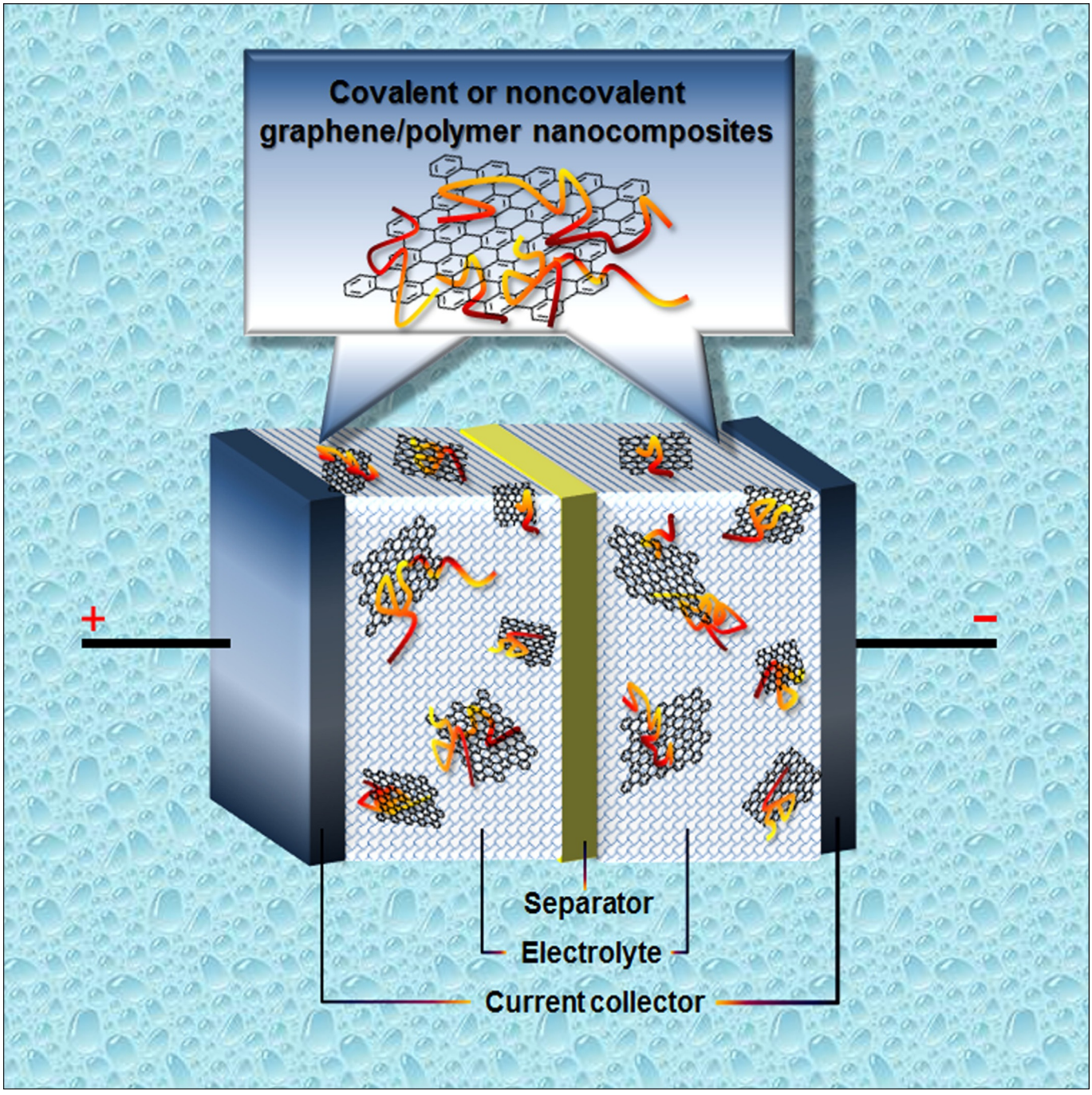

Abstract: The energy crisis and global warming are two of the greatest challenges that our society is facing nowadays, requiring an immediate solution that involves the development of clean, efficient, sustainable and cheap energy-storage devices. These energy-storage devices are highly desirable for applications in electrical vehicles, portable electronic devices, and power grids, etc. The electrochemical performance of the devices largely depends on the chemical compositions and structures of the electrode materials. Graphene/polymer hybrid nanocomposites have gained great attention as electrodes for energy storage because of their excellent mechanical, electrical and electrochemical properties, originating from the synergistic effect of the two components. In this review, we present a general overview and recent advances of graphene/polymer nanocomposites as high-performance electrode materials for supercapacitors. Major challenges to be tackled and future perspectives are also highlighted.

1. Introduction

Nowadays, highly efficient and environmentally benign energy-storage devices with reasonable costs are highly desirable in our daily life, in order to solve the two challenging issues of exhaustion of fossils fuels and climate change.[1–4] Supercapacitors, also named as electrochemical capacitors or ultracapacitors, have attracted huge attention in recent years as storage devices for applications in electrical vehicles, portable electronic devices, and power grids, etc. Based on the mechanism of energy storage, supercapacitors can be divided into two kinds: electric double-layer capacitors (EDLCs, physical absorption/desorption processes) and pseudo-capacitors (fast faradaic redox processes).[2,3,5] Supercapacitors can deliver energy in a shorter time scale with a high power density, but the energy density is usually low. The final electrochemical performance of supercapacitors is determined by several factors, including pore size distribution and geometry, specific surface area, electrical conductivity, wettability and doping of electrodes.

Hitherto, a variety of materials have been employed as electrode materials for supercapacitors, such as carbon-based materials, metal oxides, and conducting polymers, etc. Carbon-based materials have the storage mechanism of EDLCs. These materials normally have high power densities, good cycling performance but unsatisfactory energy densities. Metal oxides and conducting polymers are the typical materials showing a pseudo-capacitive behavior. These kinds of materials usually possess high specific capacitance yet limited cycling stability.

Graphene, a 2D sp^2 carbon arrangement with one-atom thickness, is appealing for supercapacitors due to its excellent electrical conductivity, large specific surface area, superior mechanical properties and good electrochemical performance.[6] When graphene is used in supercapacitors, it is often combined with other materials to further increase its electrochemical performance.[7,8]

Polymers such as polyaniline (PANI), polypyrrole (PPy), poly(3,4-ethylenedioxythiophene):poly(styrenesulfonate) (PEDOT:PSS) have already been widely employed as active electrodes for supercapacitors possessing high pseudo-capacitance.[9] However, they suffer from poor rate and cyclic stability due to swelling and shrinkage of the polymers during long term charge/discharge cycles. These problems can be solved by integrating polymers with other materials such as graphene to yield more robust functional nanocomposites.[10,11]

Recently, graphene/polymer hybrid nanocomposites have attracted tremendous attention for applications in transparent conductive coatings, catalysts, sensors, and memory devices, particularly in energy conversion and storage.[12] Hybrid systems combining graphene and polymers show obvious advantages. The nanocomposite electrodes can combine both EDLCs from graphene and pseudo-capacitance from polymers, and therefore increase the overall electrochemical performance of the nanocomposites by taking full advantage of both energy-storage mechanisms. The presence of graphene can enhance the mechanical stability and electrical conductivity of polymers. Graphene with high electrical conductivity facilitates the electron transfer during redox reactions in conducting polymers. On the other hand, polymers can act as spacers to further separate graphene sheets, they can function as surfactants to improve the dispersibility and processibility of graphene in solvents, and they can also enhance the final electrochemical performance via pseudo-capacitance effects.

In this Focus Review, the preparation methods of graphene/polymer nanocomposites will be briefly presented. The recent advances of graphene/polymer nanocomposites as high-performance electrodes for supercapacitors will be mainly discussed. Finally, the future directions of this area will be also highlighted.

2. Preparation of Graphene/Polymer Nanocomposites

Graphene can be prepared using several methods,[13] including mechanical cleavage,[14] reduction of graphene oxide,[15–18] ultrasound-induced liquid phase exfoliation (UILPE),[19–24] electrochemical exfoliation,[25,26] and chemical vapor deposition (CVD),[27,28] etc. Mechanical cleavage using scotch tape produ-

[a] Dr. X. Zhang, Prof. P. Samorì
University of Strasbourg, CNRS, ISIS UMR 7006
8 allée Gaspard Monge, F-67000 Strasbourg (France)
E-mail: samori@unistra.fr

The ORCID identification number(s) for the author(s) of this article can be found under:
https://doi.org/10.1002/cnma.201700055.

This manuscript is part of a Special Issue on 2D Materials for Energy Applications. Click here to see the Table of Contents of the special issue.

ces the highest quality graphene sample but is unsuitable for large-scale preparation. UILPE can produce a large amount of mono- and few-layer graphene flakes, however, the size of the nanosheets is limited and the content of monolayer is rather low. The CVD method can produce large-area graphene but requiring high temperature growth process and the cost is high. Electrochemical exfoliation can yield large graphene flakes with relatively low defects. Among all the methods, reduction of graphene oxide yielding reduced graphene oxide (rGO) is the most commonly used method to fabricate graphene/polymer nanocomposites.

Graphene/polymer nanocomposites can be prepared via either noncovalent or covalent approaches (Scheme 1), by tailoring the interactions between the two components.[29] The functionalization can be carried out either in a liquid media or on dry samples (e.g., ball milling).

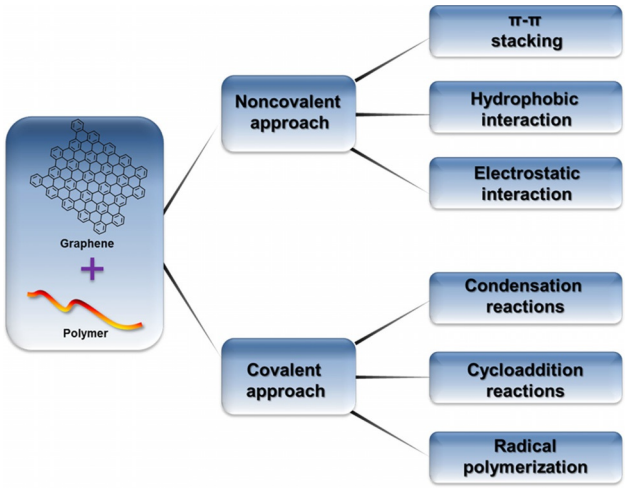

Scheme 1. Functionalization of graphene with polymers using noncovalent and covalent approaches.

2.1. Noncovalent approach

Noncovalent functionalization of graphene is carried out by physical adsorption of molecules onto graphene through π–π, hydrophobic or electrostatic interactions.[29,30] This method largely preserves the intrinsic properties of graphene: it does not alter its chemical structure, but at the same time it allows for modulation of its properties. The approach can be realized by mixing components, or via in situ polymerization of monomers in the presence of graphene. The techniques include vacuum filtration, layer-by-layer assembly, etc. Thanks to the noncovalent modification with polymers, the dispersibility and processability of graphene in solvents can be greatly improved. For example, rGO nanosheets can be stably dispersed in water in the presence of sulfonated polyaniline due to the π–π interactions between the two components.[31]

2.2 Covalent approach

Covalent functionalization of graphene with polymers can be achieved via chemical reactions, including condensation or cycloaddition reactions (grafting to: polymers with reacting groups are chemically attached onto graphene),[32,33] or radical polymerization (grafting from: chemically attached initiators on graphene to initiate polymerization),[34] etc. Compared to the noncovalent approach, covalent modification provides more stable and robust composite systems.[34–36] For instance, PANI can be chemically attached onto rGO via in situ oxidation polymerization aniline monomers in the presence of $(NH_4)_2S_2O_8$.[34]

3. Graphene/Polymer Nanocomposites for Supercapacitors

Polymers, especially conducting polymers, have received considerable attention due to their unique properties, which makes them key components for potential applications in sensors, drug carriers, electrochromic devices, and energy conversion and storage.[37] Hybrid nanocomposites combining graphene and polymers with excellent mechanical, electrical properties and large specific surface areas are particularly suitable for supercapacitor applications. For this purpose, polymers with a good electrical conductivity and a high pseudo-capacitance are generally required. Among various polymers, PANI and PPy have been the most widely used ones in combination with graphene as electrodes for high performance supercapacitors. In addition, PEDOT:PSS and other kinds of polymers were also employed. Below, we will discuss the performance of supercapacitors based on graphene with different polymers.

Dr. Xiaoyan Zhang performed his PhD in the group of Prof. Ben L. Feringa at the Stratingh Institute for Chemistry and Zernike Institute for Advanced Materials, University of Groningen, the Netherlands. He is currently a postdoctoral researcher in the group of Prof. Paolo Samorì at the Institut de Science et d'Ingénierie Supramoléculaires (ISIS) of the University of Strasbourg, France. His current research interest focuses on preparation, characterization and functionalization of 2D materials for functional nanocomposites and energy-related applications.

Paolo Samorì is Distinguished Professor and director of the Institut de Science et d'Ingénierie Supramoléculaires (ISIS) of the Université de Strasbourg (UdS). He is also Fellow of the Royal Society of Chemistry (FRSC), fellow of the European Academy of Sciences (EURASC), member of the Academia Europaea (MAE) and member of the Institut Universitaire de France (IUF). His research interests include layered materials, organic semiconductors, hierarchical self-assembly of hybrid architectures, supramolecular electronics, and the fabrication of organic- and graphene-based nanodevices. His work was awarded various prizes, including the Young Scientist Awards at E-MRS (1998) and MRS (2000), the IUPAC Prize for Young Chemists (2001), the "Vincenzo Caglioti" Award (2006) granted by the Accademia Nazionale dei Lincei (Italy), the ERC Starting Grant (2010) and the CNRS Silver Medal (2012).

3.1. Graphene/PANI

PANI itself possesses a very high theoretical specific pseudo-capacitance of 2000 $F g^{-1}$ and unique fast redox and acid–base doping/dedoping properties. High-performance supercapacitors based on graphene/PANI nanocomposites have been well-studied by many groups.[34,38–70]

In situ polymerization has been widely employed to fabricate graphene/polymer nanocomposites. Cheng and co-workers have fabricated a freestanding and flexible noncovalent graphene/PANI composite paper through an in situ anodic electrochemical polymerization of aniline monomers into a PANI film on a graphene paper.[38] The as-fabricated composite paper showed a tensile strength of 12.6 MPa, a volumetric capacitance of 135 $F cm^{-3}$ and a gravimetric capacitance of 233 $F g^{-1}$, which is very promising for flexible supercapacitors. Compared with oxidation polymerization in the solvents, composite films formed via electrochemical polymerization can be directly employed as electrodes without other binders for supercapacitors, thus avoiding the step of fabricating electrodes.

Hierarchical nanocomposites were prepared by aligning 1D PANI nanowire arrays physisorbed on GO nanosheets.[40] The morphology of PANI nanowires can be adjusted by varying the ratios between aniline monomers and GO. When used as electrode materials in supercapacitors, the hierarchical nanocomposite showed a specific capacitance of 555 $F g^{-1}$ at a low current density of 0.2 $A g^{-1}$, which is much higher than each individual component, due to a synergistic effect of PANI and GO. In another example, PANI nanowire arrays were grown on a 3D rGO film via physisorption using a dilute polymerization process to yield a hierarchical composite.[44] The composite possessed a specific capacitance of 385 $F g^{-1}$ at a current density of 0.5 $A g^{-1}$, with a capacitance retention of 88% over 5000 cycles. When the supercapacitor was bent by 90° and 180°, no obvious changes in the cyclic voltammetry (CV) curves were observed, indicating the performance is stable at different bending states (Figure 1). The flexible hierarchical composite proves to be a good electrode material for flexible or rolled-up devices.

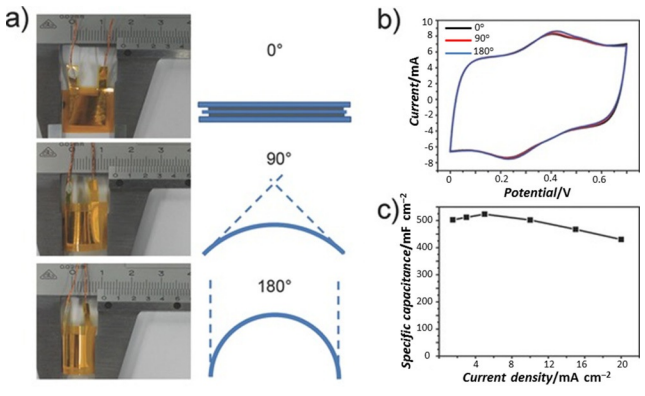

Figure 1. a) Images and schematics of the flexible supercapacitor based on 3D rGO/PANI nanowire arrays at different bending states: 0°, 90°, and 180°. b) CV curves of the film supercapacitor at a scan rate of 20 $mV s^{-1}$ when the device was bent by 0°, 90°, 180°. c) Area specific capacitance of the flexible supercapacitor at different current densities. Reproduced with permission from ref. [44]. Copyright 2013, Wiley-VCH Verlag GmbH & Co. KGaA, Weinheim.

Li et al. fabricated hierarchical nanostructured materials consisting of stacked PANI nanowire forests noncovalently interconnected by monolayer graphene sheets using a bottom-up nanofabrication process.[45] The as-prepared hierarchical nanostructures were used as supercapacitor electrodes, showing a specific energy density as high as 137 $Wh kg^{-1}$ and a power density of 1980 $W kg^{-1}$ for the three-stacked nanostructured electrode. This work demonstrated a simple pathway to tailor electrode architecture for supercapacitors with excellent electrochemical performance. Recently, PANI/rGO composites with a macroscopically phase-separated structure were prepared via electrochemical deposition of PANI physically absorbed outside the rGO hydrogel.[50] The composite electrode exhibited a high specific capacitance of 783 $F g^{-1}$ (8773 $mF cm^{-2}$) at a high current density of 27.3 $A g^{-1}$ (305.7 $mA cm^{-2}$), which is 99% of the value at a current density of 1.14 $A g^{-1}$, demonstrating an excellent rate performance. The authors attributed that the phase-separated structure is beneficial to the diffusion of electrolyte, thus can significantly improve the electrochemical performance of the composites.

Physical mixing of graphene and polymers in a given solvent is another commonly used method since it is simple and enables facile solution processing. Layered composite films were prepared by vacuum filtration of the mixed dispersions of both rGO and PAIN nanofibers.[39] The film was mechanically stable and showed a good flexibility. When tested in supercapacitor devices the composite film showed large electrochemical capacitance of 210 $F g^{-1}$ at a low discharge rate of 0.3 $A g^{-1}$.

Currently available printing techniques allow direct deposition of electrode materials from inks. As a good example, a series of nano graphene platelet/PANI inks with different weight ratios were prepared by a mixing process.[46] These inks were further used to produce thin-film electrodes by screen printing, which possesses the advantages of being inexpensive, rapid and capable of a large-scale production. Supercapacitors were fabricated based on these electrodes, showing a specific capacitance of 269 $F g^{-1}$ at a scan rate of 20 $mV s^{-1}$, a power density of 454 $kW kg^{-1}$ and an energy density of 9.3 $Wh kg^{-1}$, with no obvious capacitance loss over 1000 cycles. This work demonstrates an important step towards the industrial application of printable supercapacitors. Other techniques such as inkjet printing, spray coating and roll-to-roll printing can be also used to fabricate electrodes from inks. However, uniformity, mechanical stability and adhesion ability to substrates of the formed films must be optimized for a large-scale production.

Interestingly, Lai et al. studied in detail the effect of graphene surface chemistry on the electrochemical performance of graphene/PANI composites as supercapacitor electrodes.[42] GO, rGO, nitrogen-doped rGO and amine-modified rGO were used as carriers and loaded with PANI through noncovalent interactions. The surface chemistry indeed played an important role in the growth of PANI that further influenced the final specific capacitance. Under a three-electrode configuration, the amine-modified rGO showed the largest increase in specific ca-

pacitance with a value as high as 500 F g^{-1} at a very low scan rate of 2 mV s^{-1} and a factor of 1.19 increase in capacitance over 680 cycles. When nitrogen-doped rGO and amine-modified rGO/PANI were used as the cathode material and the anode material, respectively, the supercapacitor cell showed a specific capacitance of 79 F g^{-1}. This research highlights the importance of graphene surface chemistry in determining the final electrochemical performance.

Asymmetric supercapacitors can be operated at higher cell voltages than symmetric supercapacitors, and can largely increase the energy densities at the same time maintaining the power densities. An asymmetric supercapacitor was fabricated by using rGO-RuO_2 and rGO-PANI (prepared via in situ polymerization of aniline monomers in the presence of rGO) as the anode and cathode, respectively.[41] The asymmetric supercapacitor showed a more than two-fold increase in energy density compared with the symmetric supercapacitors using rGO-RuO_2 or rGO-PANI as the electrodes. The improvement in electrochemical performance can be attributed to the wider potential window in the aqueous electrolyte.

The current trend of miniaturization of electronic devices leads to a big demand for microscale energy storage devices with smaller sizes and high energy densities. Micro-supercapacitors hold the potential to fulfil the energy requirements of miniaturized flexible electronic devices on chips. Cao and coworkers reported a wet chemical approach to deposit PANI nanorods physisorbed on the thin films of patterned rGO, which was used to fabricate a flexible solid state micro-supercapacitor device.[43] The structures of the PANI nanorods can be adjusted by modifying the concentration of aniline monomers in the solution and the deposition time of the in situ electrochemical polymerization step. The micro-supercapacitor showed a high specific capacitance of 970 F g^{-1} at a current density of 2.5 A g^{-1}, and a capacitance retention of 90% over 1700 cycles.

Efforts have been also devoted to fabricate multicomponent graphene/polymer-based nanocomposites. A ternary nanocomposite consisting of vertically aligned tunable PANI and rGO/zirconium oxide has been prepared by Giri et al.[47] The morphology and the alignment of the physisorbed PANI can be tuned by simply changing the ratio of aniline monomers to graphene/ZrO_2, and also the polymerization time. The nanocomposites showed a specific capacitance of 1178.6 F g^{-1} at a current density of 0.3 A g^{-1}, an energy density of 104.76 Wh kg^{-1} and a power density of 0.8 kW kg^{-1}, with a capacitance retention of ≈93% over 1000 cycles. The vertically aligned PANI can easily contact with electrolyte ions and provides numerous redox active sites during the charging and discharging process.

In another study, a hierarchical nanostructured PANI-rGO/cellulose fibers (CF) composite paper was prepared via "dipping and drying" using a hydrothermal treatment.[48] Two redox peaks can be seen in the CV curve of the PANI-rGO/CF paper sample (Figure 2a), coming from the faradic reaction of PANI. The PANI-rGO/CF paper with a PANI deposition time of 72 h exhibited a specific capacitance of 464 F g^{-1} at a current density of 1 A g^{-1}, being greater than the nanostructured rGO/CF paper and compact rGO/CF paper (Figure 2b). Further increase of the physisorbed PANI deposition time resulted in a drop of the specific capacitance for the PANI-rGO/CF paper, due to the lower specific surface area and reduced electrical conductivity (Figure 2d). In contrast to the compact rGO/CF composite paper, the nanostructured rGO/CF composite paper displayed a less abrupt drop in specific capacitance when the scan rate was increased (Figure 2c), and the porous structure of the nanostructured rGO/CF paper can effectively inhibit the rGO sheets from aggregation and facilitate ion diffusion (Figure 2e and 2f). Flexible and foldable all-solid-state supercapacitors were fabricated using the PANI-rGO/CF composite paper, showing a specific capacitance of 224 F g^{-1} at a low current density of 0.1 A g^{-1}, with a capacitance retention of ≈89% over 1000 cycles.

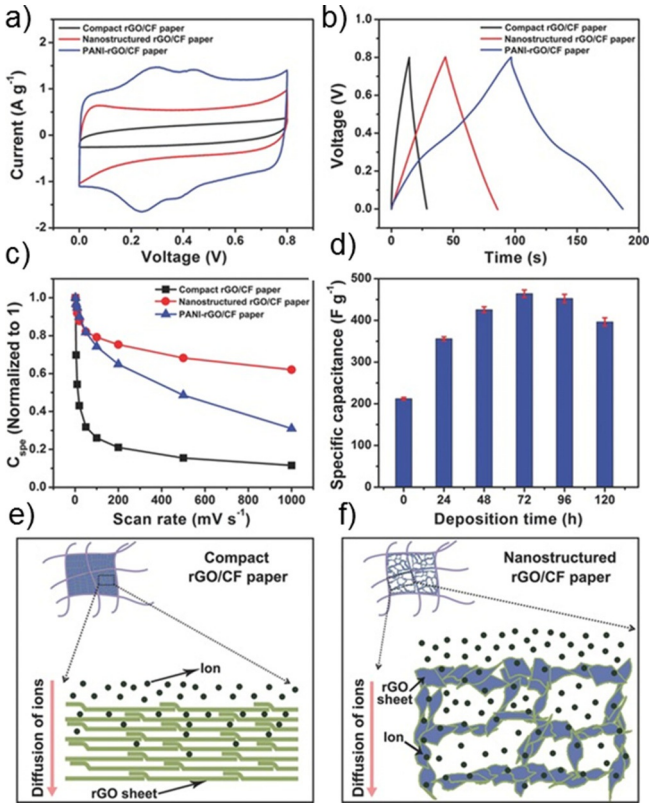

Figure 2. a) CV plots recorded at a scan rate of 10 mV s^{-1} and b) galvanostatic charge/discharge plots of supercapacitors using PANI-rGO/CF paper (PANI deposition time: 72 h), compact rGO/CF paper, and nanostructured rGO/CF paper at a current density of 1 A g^{-1}. c) Comparison of the normalized specific capacitance of PANI-rGO/CF composite paper (the deposition time of PANI was 72 h), compact rGO/CF paper, and nanostructured rGO/CF paper at different scan rates. d) Specific capacitance of the PANI-rGO/CF papers using different PANI deposition time. Scheme of ion diffusion path for e) the compact rGO/CF paper sample and f) the nanostructured rGO/CF paper sample. Reproduced with permission from ref. [48]. Copyright 2014, Wiley-VCH Verlag GmbH & Co. KGaA, Weinheim.

Textiles are porous, flexible and stretchable, making them suitable for wearable electronic devices. A rGO/PANI supercapacitor textile was fabricated by using a wet chemical and printing-based route.[49] A polyester textile was first immersed into a GO dispersion, followed by a chemical reduction step to form rGO/polyester composite textile. PANI was further physi-

cally deposited onto the textile through an in situ polymerization process. Silver paste (as current collector) was then deposited on the textile using screen printing. Remarkably, the designed supercapacitor textile system can even reach an effective area of 100 cm^2, showing a remarkable capacitance (69.3 F), power (80.7 mW), and energy (5.4 mW h), representing an important step towards real-world applications. The method can be potentially extended to other textile-based energy devices such as batteries and solar cells.

3.2 Graphene/polypyrrole (PPy)

PPy is emerging as a promising electrode material for supercapacitors due to its facile synthesis and processing, low cost, environmental stability, high mechanical flexibility, and high pseudo-capacitance. During the past few years, graphene/PPy nanocomposites have been often employed as electrodes for supercapacitors.[71–85]

Several graphene derivatives including GO, rGO, NH_2-modified rGO and N-doped rGO were prepared, and were further physically combined with PPy as electrodes for supercapacitors to systematically investigate the effect of surface functionalization on the electrochemical performance.[71] N-doped rGO/PPy electrode showed a specific capacitance of 394 F g^{-1}, which is larger than those of NH_2-modified rGO/PPy (225 F g^{-1}), GO/PPy (165 F g^{-1}), rGO/PPy electrodes (150 F g^{-1}) under the same measurement conditions. N-doping of graphene is believed to enhance electronic transfer efficiency and improve surface wettability, therefore leading to the highest electrochemical performance.

Compression, a reversible process in contrast to stretching, is one of the most common parameters used to evaluate the electrochemical performance of flexible supercapacitors under external forces. Qu and co-workers fabricated a highly compressible supercapacitor using 3D noncovalent rGO/PPy foam as electrodes (Figure 3 a).[72] The as-prepared foam was durably tolerant to large compressive strains without any structural collapse or loss of springiness (Figure 3 b). Highly compression-tolerant supercapacitors based on the deformable foam electrodes achieved a specific capacitance of 360 F g^{-1} at a current density of 1.5 A g^{-1}, a good compression tolerance without obvious changes in capacity over 1000 compressive loading and unloading cycles (Figure 3 c). This work indeed gave a good example of fabricating advanced supercapacitor devices exhibiting excellent tolerance to harsh conditions such as mechanical compression and concussion.

Graphene/PPy hybrid composites were prepared by electrochemical deposition of PPy physisorbed on porous nanotubular graphene, which was grown on a nanoporous nickel scaffold via a CVD approach.[73] The bicontinuous nanotubular hybrid material was employed as free standing electrodes in supercapacitors, showing a specific capacitance of 509 F g^{-1} at a low current density of 0.15 A g^{-1}. Furthermore, all-solid-state flexible supercapacitors fabricated using the hybrid material and PVA/H_2SO_4 gel electrolyte showed a specific capacitance of 514 F g^{-1} at a low current density of 0.2 A g^{-1}, an energy density of 21.6 Wh kg^{-1} and a power density of 32.7 kW kg^{-1}. In another case,[76] a flexible rGO/PPy composite paper was prepared by physically mixing GO and PPy, followed by vacuum filtration and chemical reduction. The as-fabricated rGO/PPy composite paper was directly used as binder-free electrodes for supercapacitors, showing an areal capacitance of 175 mF cm^{-2} at a low scan rate of 10 mV s^{-1}, with a capacitance retention of 93 % over 5000 cycles.

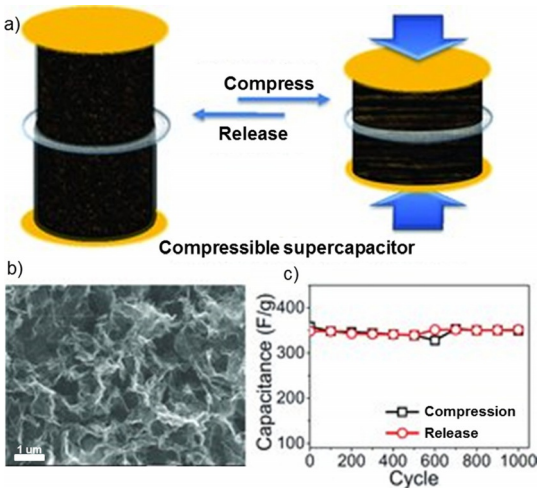

Figure 3. a) Scheme of 3D rGO/PPy foam-based compressible supercapacitor. b) Scanning electron microscopy (SEM) image of 3D rGO/PPy foam under unloading status. c) The specific capacitance under compression/release conditions over 1000 cycles. Reproduced with permission from ref. [72]. Copyright 2013, Wiley-VCH Verlag GmbH & Co. KGaA, Weinheim.

3.3 Graphene/(PEDOT:PSS)

PEDOT:PSS shows good electrical conductivity, transparency, ductility, and stability, and have been widely used in energy conversion and storage devices such as solar cells, fuel cells, supercapacitors, thermoelectric devices and stretchable devices.[86] PEDOT:PSS can have electrostatic interactions with graphene to form nanocomposites as electrodes for supercapacitors.[87–91]

Wu et al. demonstrated ultrathin printable supercapacitors based on solution-processed electrochemically exfoliated graphene/(PEDOT:PSS) hybrid conductive ink (prepared via physical mixing) spray coated on an ultrathin poly(ethylene terephthalate) (PET) substrate.[87] The supercapacitor devices exhibited a very large volumetric capacitance of 348 F cm^{-3}, an ultrahigh scan rate of 2000 V s^{-1}, an excellent capacitance retention ability over 50 000 cycles, a good flexibility under different bending states and alternating current (AC) line-filtering performance with an ultrashort resistor-capacitor (RC) time constant of <0.5 ms. The present method can be potentially used for large-scale production of printable, thin and lightweight supercapacitor devices.

Fiber-shaped supercapacitors have gained increasing attention because of their tiny volume, low weight, high flexibility, and good wearability. A hollow noncovalent rGO/PEDOT:PSS composite fiber has been fabricated inside a glass pipe.[88] The fiber showed high mechanical and electronic properties and

was used to fabricate novel fiber-shaped supercapacitors that displayed a high specific capacitance of 304.5 mF cm^{-2} at 0.08 mA cm^{-2} (Figure 4a), an energy density of 27.1 μW h cm^{-2}, and a long life stability over 10^4 cycles (Figure 4b). The curve

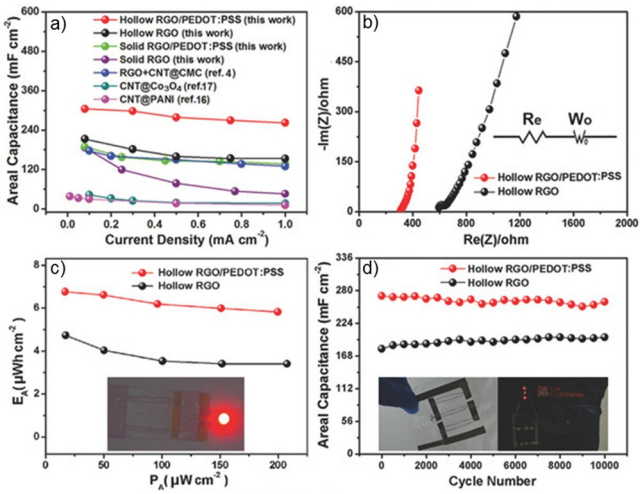

Figure 4. a) Comparison of area specific capacitance of hollow rGO/PEDOT:PSS composite fiber with other samples at different current densities. b) Electrochemical impedance spectroscopy (EIS) of hollow rGO/PEDOT:PSS composite and hollow rGO. c) Ragone plots based on the whole fiber supercapacitors using hollow rGO/PEDOT:PSS composite and hollow rGO. The inset image shows that a serial fiber supercapacitor is lighting up a red light-emitting diode (LED). d) Cycling performance of the entire fiber supercapacitors using hollow rGO/PEDOT:PSS composite and hollow rGO. The inset image shows that three fiber supercapacitors are connected in series and stuck onto clothes to supply power to three LEDs. In the Figure, RGO stands for rGO. Reproduced with permission from ref. [88]. Copyright 2016, Wiley-VCH Verlag GmbH & Co. KGaA, Weinheim.

of Ragone plots for the hollow rGO/PEDOT:PSS composite was relatively flat, suggesting that the high energy density of the fiber supercapacitor was retained with increasing power output (Figure 4c). The equivalent series resistance (ESR) value of hollow rGO/PEDOT:PSS is much lower than hollow rGO, indicating higher electrical conductivity of the rGO/PEDOT:PSS sample (Figure 4b). Moreover, the fiber showed an electrical conductivity of 4700 S m^{-1}. The fiber supercapacitors can be woven into flexible powering textiles which can maintain their electrochemical performance after cycling and bending, which is particularly promising for portable and wearable electronic devices.

3.4 Graphene/other polymers

Alongside the above-discussed commonly used polymers, other polymers have been also combined with graphene as electrodes for supercapacitor devices.[92–104]

Graphene-based 3D covalent networks (G3DCNs) with adjustable interlayer distance were prepared by reacting benzidines with graphene oxide at three different reaction temperatures without addition of any catalyst or template (Figure 5).[92] The chemically reduced G3DCNs samples were tested as electrodes in supercapacitor devices. Using a two-electrode cell,

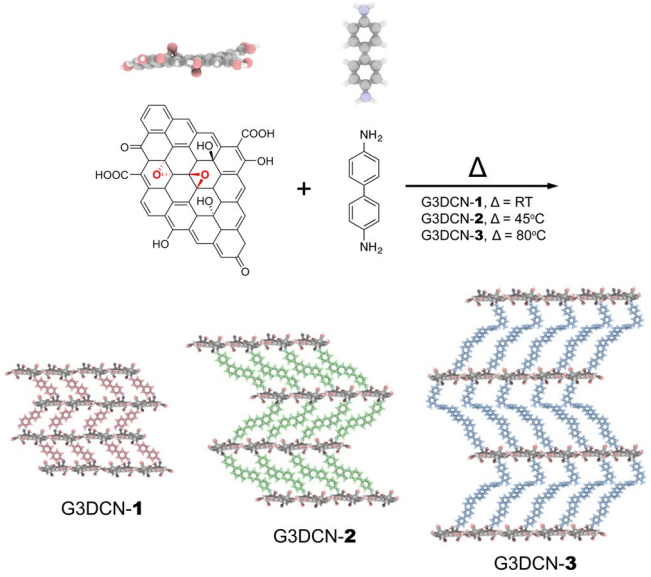

Figure 5. Preparation of graphene-based 3D covalent networks (G3DCNs) with adjustable interlayer distance by reacting benzidines with graphene oxide at three different reaction temperatures. Reproduced with permission from ref. [92]. Copyright 2016, Wiley-VCH Verlag GmbH & Co. KGaA, Weinheim.

the reduced form of G3DCNs-**3** showed the highest specific capacitance of ≈156 F g^{-1} at a current density of 1 A g^{-1}, with no obvious capacitance loss over 5000 cycles. G3DCNs-**3** possessed the highest specific surface area and nitrogen content, leading to the highest electrochemical performance, even though its electrical conductivity was the lowest. The study gives a good example of smart design of graphene-based 3D functional nanocomposites, and helps to better understanding of structure–property relationship.

Conjugated polyfluorene imidazolium ionic liquids (PILs) noncovalently modified rGO composites were used as electrodes for high-performance supercapacitors.[93] Two polyfluorene homo-polymer (hoPIL) and co-polymer (co-PIL) with hexyl imidazolium bromide side chains were synthesized. In the three-electrode configuration, the coPIL-rGO showed a specific capacitance of 222 F g^{-1} at a low current density of 0.2 A g^{-1} in 6 M KOH and 132 F g^{-1} at a current density of 0.5 A g^{-1} in ionic liquid electrolyte 1-butyl-3-methylimidazolium tetrafluoroborate ($BMIMBF_4$), respectively. When assembled into a symmetric two-electrode cell using BMIMBF4/acetonitrile (1:1) as the electrolyte, the coPIL-rGO exhibited an energy density of 14.7 Wh kg^{-1} at a current density of 0.5 A g^{-1}. While a power density of 347 kW kg^{-1} was obtained for hoPIL-rGO at a current density of 5 A g^{-1}. This study highlights the importance of polymer structure in affecting the electrochemical properties.

Due to their widespread availability, low cost, excellent mechanical strength and flexibility, cellulose papers are particularly appealing in flexible energy storage devices. rGO-cellulose paper membranes were fabricated using simple vacuum filtration of a rGO dispersion through a filter paper.[94] rGO can penetrate into the filter paper, forming a continuous physisorbed conducting network around the cellulose fibers. By absorbing electrolyte, the cellulose fibers in the filter paper can function

as electrolyte reservoirs to largely facilitate ion transport during electrochemical process. The as-formed membranes were used as freestanding and binder-free electrode materials for flexible supercapacitor devices, showing a specific area capacitance of 81 mF cm^{-2} and capacitance retention of >99% over 5000 cycles. When the whole supercapacitor device was bent in a large angle, it still exhibited a specific area capacitance of 46 mF cm^{-2}. These results clearly demonstrated that supercapacitors based on graphene and filter paper are quite versatile and can be applicable in flexible, wearable, and portable microelectronic devices.

Noncovalent rGO-polyselenophene nanocomposites were prepared using an in situ oxidation polymerization method between GO and selenophene monomers.[99] The as-prepared nanocomposites showed a high specific surface area, good electrical conductivity and remarkable mechanical properties. As a proof of concept, an all-solid-state supercapacitor was fabricated. Using H_2SO_4-PVA gel as the solid electrolyte, the device exhibited a specific capacitance of ≈293 F g^{-1} before bending, and ≈288 F g^{-1} after bending at a current density of 4 A g^{-1}, in line with the CV measurement (Figure 6), indicating a stable electrochemical performance as flexible energy storage devices.

The above discussed preparation methods can be extended to new interesting polymer candidates combined with graphene as electrodes for supercapacitors. The most widely used method is the noncovalent approach, while few examples of using covalently linked graphene/polymer nanocomposites in supercapacitors have been reported.[34,92,103] This is reasonable, as supercapacitor cells require electrode materials with a high electrical conductivity, and the noncovalent method can largely reserve the intrinsic properties of graphene therefore leading to a high electrical conductivity of the formed nanocomposites. However, proper design of nanocomposites with good electrical conductivity by delicate covalent modification of graphene using polymers still holds a great potential for high-performance supercapacitor applications. For example, covalent

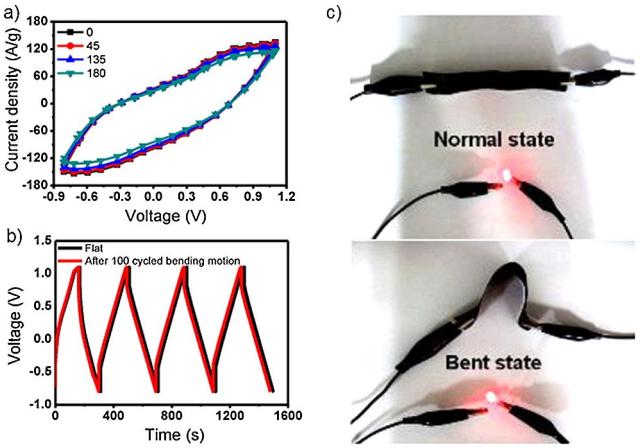

Figure 6. All-solid-state supercapacitor based on graphene-polyselenophene nanocomposites. a) CV plots recorded at a scan rate of 200 mV s^{-1} at different bending states and b) galvanostatic charge–discharge plots at a current density of 4 A g^{-1} before (black curve) and after 100 bending cycles (red curve). c) The supercapacitor was used to power a LED under normal and bent states. Reproduced with permission from ref. [99]. Copyright 2014, American Chemical Society (ACS).

functionalization of GO using polymers through ring-opening and condensation reactions followed by a chemical reduction step to yield rGO/polymers nanocomposites is a very promising route to realize supercapacitor devices with good electrochemical performance.[92] The electrochemical performance of some of the graphene/polymer nanocomposites is summarized in Table 1. Graphene has a low packing density, leading to a low volumetric specific capacitance of the hybrid nanocomposites. Also, the energy density of the nanocomposites is still not high for practical applications.

4. Conclusions and Outlook

In the present review, the preparation method and recent progress of graphene/polymer nanocomposites for supercapa-

Table 1. Summary of supercapacitor performance of graphene/polymer nanocomposites.

Ref.	Electrode compositions	Electrolyte	Capacitance, energy/power density	Cycling stability
[43]	PANI nanorod arrays on patterned rGO thin films	H_3PO_4-polyvinyl alcohol (PVA) gel electrolyte	970 F g^{-1} at 2.5 A g^{-1}	90% retained over 1700 cycles
[44]	rGO/PANI nanowires	1 M H_2SO_4	385 F g^{-1} at 0.5 A g^{-1}	88% retained over 5000 cycles
[46]	Nano graphene platelet/PANI	1 M H_2SO_4	269 F g^{-1} at 20 mV s^{-1}, 454 kW kg^{-1} and 9.3 Wh kg^{-1}	Stable over 1000 cycles
[48]	PANI-rGO/cellulose fibers	H_2SO_4-polyvinylacetate (PVA) gel electrolyte	224 F g^{-1} at 0.1 A g^{-1}	89% retained over 1000 cycles
[72]	3D rGO/PPy foam	3 M $NaClO_4$	360 F g^{-1} at 1.5 A g^{-1}	No change over 1000 compression/release cycles
[87]	Electrochemically exfoliated graphene/(PEDOT:PSS)	H_2SO_4-polyvinylacetate (PVA) gel electrolyte	348 F cm^{-3}	Stable over 50 000 cycles
[88]	rGO/PEDOT:PSS composite fiber	H_3PO_4-polyvinyl alcohol (PVA) gel electrolyte	304.5 mF cm^{-2} at 0.08 mA cm^{-2}, 27.1 μW h cm^{-2}	Stable over 10^4 cycles
[92]	3D polymerized benzidines covalently linked rGO	1 M H_2SO_4	156 F g^{-1} at 1 A g^{-1}	No obvious loss over 5000 cycles
[94]	rGO-cellulose paper	H_2SO_4-polyvinylacetate (PVA) gel electrolyte	81 mF cm^{-2}	>99% over 5000 cycles
[99]	rGO-polyselenophene	H_2SO_4-polyvinylacetate (PVA) gel electrolyte	293 F g^{-1} at 4 A g^{-1}	98.4% retained after 100 bending cycles

citors have been summarized. The nanocomposites show enhanced electrochemical performance in supercapacitor devices due to the synergetic effects of graphene and polymers from combining the unique properties of the individual components. Although much progress has been made in this area, there are still quite a few challenges to be tackled in the future.

There is still inconsistency in the evaluation method for supercapacitors; either two- and/or three-electrode configurations have been used for electrochemical measurements. For reliable measurements reflecting practical commercial applications, it is recommended to use a two-electrode configuration to test electrode materials following the industrial test standards and procedures. Also, test cells should have active materials with mass loadings on the order of 10 mg cm^{-2}.[92, 105] When one compares the supercapacitor performances reported in literature, they also need to consider other parameters such as electrolytes, electrode compositions, mass loading, potential windows, electrode configuration, all of which can affect the final capacitance. For graphene/polymer-nanocomposites-based supercapacitors, volumetric specific capacitance is a more reliable indicator to evaluate their electrochemical performance when the total device volume is considered.

Currently, supercapacitors have high power densities but still suffer from lower energy densities. The low ionic conductivities (especially solid electrolytes for flexible supercapacitors and organic electrolytes) and narrow potential windows of electrolytes limit the supercapacitor performance in both power density and energy density. This problem can be solved by using novel electrolytes with high ionic conductivities and larger electrochemical potential windows. Recently, new efforts have already been devoted to fabricate hybrid energy storage devices such as lithium/sodium-ion hybrid capacitors,[106, 107] composed of both battery-type electrodes and capacitor-type electrodes, which can possess both high energy and power density.

The electrochemical performance of graphene/polymer nanocomposites depends very much on how the two components interact and on the resulting structures/morphologies. In this regard, optimization of the structure and interface of electrode materials is imperative, in order to provide more electroactive sites and largely enhance the kinetics of ion transport. One of the main goals in designing new electrode materials is to improve their rate performance at high current densities, which requires electrode materials with high electrical conductivity. However, as the most widely used graphene derivative for the preparation of graphene/polymer nanocomposites, rGO still contains a lot of defects, which reduces the electrical conductivity of the final nanocomposites. Electrochemical exfoliation of graphene with a few defects could be a better alternative to replace rGO. The CVD method can provide much higher-quality samples; however, much effort is needed to produce CVD graphene in a large scale and with a reasonable cost. More interesting polymers need to be further designed/synthesized to fabricate novel functional graphene-based nanocomposites, which can lead to much better electrochemical performance. The preparation methods employed to generate graphene/polymer nanocomposites also plays an important role in determining the structures/morphologies. Among the currently used methods, in situ polymerization and physical mixing appear to hold the most promise towards large-scale production of graphene/polymer nanocomposites. Besides the already well-established procedures reported in literature, novel preparation routes still need to be developed to fabricate advanced nanocomposites with superior electrochemical performance.

Homogeneous dispersion of graphene within the polymer matrix is necessary but it is still a challenging goal.[108] Graphene itself has a strong tendency towards aggregation during processing mainly due to the strong π–π interactions between the individual sheet, thus largely lowering the specific surface area and leading to a lower electrochemical performance. A possible appealing solution is to build 3D graphene/polymer hybrids with controlled/tunable structures possessing large specific surface area and good permeability.[92]

Furthermore, deeper understanding of the mechanism of energy storage, the interfacial interactions between the electrode and electrolyte, and the structure–electrochemical performance relationships is highly desired.[109] All these will require in situ experimental characterization techniques combined with theoretical calculations.

New types of supercapacitor devices such as micro-supercapacitors and fiber-type supercapacitors have been widely demonstrated, which can meet the energy requirements of the next generation of smart electronic devices. Pushing further the size limit of micro-supercapacitors is needed towards more advanced on-chip microelectronic devices. 3D printing could be very a useful technique for the fabrication of micro-supercapacitors. Nowadays, developing free-standing, flexible supercapacitors that can retain excellent electrochemical performance under external mechanical deformation such as bending, twisting, stretching and compression, and/or against harsh environments such as very low/high temperatures or stress, is one of the hottest directions in flexible electronics. Safe operation should always be seriously taken into account especially for applications in wearable electronic devices and smart textiles. Integrated multifunctional systems combining supercapacitor devices with other kinds of energy-harvesting or energy-storage devices, such as solar cells, batteries, nanogenerators, or electrochromic devices to realize energy conversion and storage in a single unit,[110] is an emerging direction to fabricate advanced smart-energy devices.

With the continuous efforts on the research of graphene/polymer nanocomposites for supercapacitors, it is anticipated that the above-discussed issues could be solved properly in the coming decades. Importantly, a closer joint effort between lab research and industry is highly desired to solve the challenges together and thus fulfil the ultimate goal of large-scale fabrication of supercapacitors using graphene/polymer nanocomposites. This will finally lead to generating more-advanced clean, efficient and renewable storage devices towards practical applications in our daily life.

Acknowledgements

This work was supported by the European Commission through the Graphene Flagship – Core 1 project (GA-696656) and the ANR through the LabEx CSC (ANR-10-LABX-0026 CSC), the International Center for Frontier Research in Chemistry (icFRC). Dr. Lili Hou is thanked for the help with drawing the images.

Conflict of interest

The authors declare no conflict of interest.

Keywords: graphene · nanocomposites · polymer · supercapacitors

[1] M. R. Lukatskaya, B. Dunn, Y. Gogotsi, *Nat. Commun.* **2016**, *7*, 12647.
[2] X. Y. Zhang, L. L. Hou, A. Ciesielski, P. Samorì, *Adv. Energy Mater.* **2016**, *6*, 1600671.
[3] F. Bonaccorso, L. Colombo, G. Yu, M. Stoller, V. Tozzini, A. C. Ferrari, R. S. Ruoff, V. Pellegrini, *Science* **2015**, *347*, 1246501.
[4] L. Dai, D. W. Chang, J. B. Baek, W. Lu, *Small* **2012**, *8*, 1130 – 1166.
[5] P. Simon, Y. Gogotsi, *Nat. Mater.* **2008**, *7*, 845 – 854.
[6] A. C. Ferrari, F. Bonaccorso, V. Fal'ko, K. S. Novoselov, S. Roche, P. Boggild, S. Borini, F. H. Koppens, V. Palermo, N. Pugno, J. A. Garrido, R. Sordan, A. Bianco, L. Ballerini, M. Prato, E. Lidorikis, J. Kivioja, C. Marinelli, T. Ryhanen, A. Morpurgo, J. N. Coleman, V. Nicolosi, L. Colombo, A. Fert, M. Garcia-Hernandez, A. Bachtold, G. F. Schneider, F. Guinea, C. Dekker, M. Barbone, Z. Sun, C. Galiotis, A. N. Grigorenko, G. Konstantatos, A. Kis, M. Katsnelson, L. Vandersypen, A. Loiseau, V. Morandi, D. Neumaier, E. Treossi, V. Pellegrini, M. Polini, A. Tredicucci, G. M. Williams, B. H. Hong, J. H. Ahn, J. M. Kim, H. Zirath, B. J. van Wees, H. van der Zant, L. Occhipinti, A. Di Matteo, I. A. Kinloch, T. Seyller, E. Quesnel, X. Feng, K. Teo, N. Rupesinghe, P. Hakonen, S. R. Neil, Q. Tannock, T. Lofwander, J. Kinaret, *Nanoscale* **2015**, *7*, 4598 – 4810.
[7] Y. B. Tan, J.-M. Lee, *J. Mater. Chem. A* **2013**, *1*, 14814 – 14843.
[8] J. Zhu, D. Yang, Z. Yin, Q. Yan, H. Zhang, *Small* **2014**, *10*, 3480 – 3498.
[9] J. Kim, J. Lee, J. You, M.-S. Park, M. S. A. Hossain, Y. Yamauchi, J. H. Kim, *Mater. Horiz.* **2016**, *3*, 517 – 535.
[10] J. Zhang, X. S. Zhao, *J. Phys. Chem. C* **2012**, *116*, 5420 – 5426.
[11] M. A. Memon, W. Bai, J. Sun, M. Imran, S. N. Phulpoto, S. Yan, Y. Huang, J. Geng, *ACS Appl. Mater. Interfaces* **2016**, *8*, 11711 – 11719.
[12] L. Wang, X. Lu, S. Lei, Y. Song, *J. Mater. Chem. A* **2014**, *2*, 4491 – 4509.
[13] F. Bonaccorso, A. Lombardo, T. Hasan, Z. Sun, L. Colombo, A. C. Ferrari, *Mater. Today* **2012**, *15*, 564 – 589.
[14] K. S. Novoselov, A. K. Geim, S. V. Morozov, D. Jiang, Y. Zhang, S. V. Dubonos, I. V. Grigorieva, A. A. Firsov, *Science* **2004**, *306*, 666 – 669.
[15] S. Pei, H.-M. Cheng, *Carbon* **2012**, *50*, 3210 – 3228.
[16] J. M. Mativetsky, E. Treossi, E. Orgiu, M. Melucci, G. P. Veronese, P. Samorì, V. Palermo, *J. Am. Chem. Soc.* **2010**, *132*, 14130 – 14136.
[17] J. M. Mativetsky, A. Liscio, E. Treossi, E. Orgiu, A. Zanelli, P. Samorì, V. Palermo, *J. Am. Chem. Soc.* **2011**, *133*, 14320 – 14326.
[18] E. Kymakis, K. Savva, M. M. Stylianakis, C. Fotakis, E. Stratakis, *Adv. Funct. Mater.* **2013**, *23*, 2742 – 2749.
[19] V. Nicolosi, M. Chhowalla, M. G. Kanatzidis, M. S. Strano, J. N. Coleman, *Science* **2013**, *340*, 1226419.
[20] X. Y. Zhang, A. C. Coleman, N. Katsonis, W. R. Browne, B. J. van Wees, B. L. Feringa, *Chem. Commun.* **2010**, *46*, 7539 – 7541.
[21] W. F. van Dorp, X. Y. Zhang, B. L. Feringa, J. B. Wagner, T. W. Hansen, J. T. M. De Hosson, *Nanotechnology* **2011**, *22*, 505303.
[22] A. Ciesielski, P. Samorì, *Chem. Soc. Rev.* **2014**, *43*, 381 – 398.
[23] A. Ciesielski, P. Samorì, *Adv. Mater.* **2016**, *28*, 6030 – 6051.
[24] W. F. van Dorp, X. Y. Zhang, B. L. Feringa, T. W. Hansen, J. B. Wagner, J. T. M. De Hosson, *ACS Nano* **2012**, *6*, 10076 – 10081.
[25] S. Yang, M. R. Lohe, K. Müllen, X. Feng, *Adv. Mater.* **2016**, *28*, 6213 – 6221.
[26] Z. Y. Xia, S. Pezzini, E. Treossi, G. Giambastiani, F. Corticelli, V. Morandi, A. Zanelli, V. Bellani, V. Palermo, *Adv. Funct. Mater.* **2013**, *23*, 4684 – 4693.
[27] X. Li, W. Cai, J. An, S. Kim, J. Nah, D. Yang, R. Piner, A. Velamakanni, I. Jung, E. Tutuc, S. K. Banerjee, L. Colombo, R. S. Ruoff, *Science* **2009**, *324*, 1312 – 1314.
[28] J. Sun, Y. Zhang, Z. Liu, *ChemNanoMat* **2016**, *2*, 9 – 18.
[29] X. Y. Zhang, L. L. Hou, P. Samorì, *Nat. Commun.* **2016**, *7*, 11128.
[30] X. Y. Zhang, E. H. Huisman, M. Gurram, W. R. Browne, B. J. van Wees, B. L. Feringa, *Small* **2014**, *10*, 1735 – 1740.
[31] H. Bai, Y. Xu, L. Zhao, C. Li, G. Shi, *Chem. Commun.* **2009**, 1667 – 1669.
[32] D. Yu, Y. Yang, M. Durstock, J.-B. Baek, L. Dai, *ACS Nano* **2010**, *4*, 5633 – 5640.
[33] B. Zhang, G. Liu, Y. Chen, L.-J. Zeng, C.-X. Zhu, K.-G. Neoh, C. Wang, E.-T. Kang, *Chem. Eur. J.* **2011**, *17*, 13646 – 13652.
[34] N. A. Kumar, H.-J. Choi, Y. R. Shin, D. W. Chang, L. Dai, J.-B. Baek, *ACS Nano* **2012**, *6*, 1715 – 1723.
[35] X. Y. Zhang, L. L. Hou, A. Cnossen, A. C. Coleman, O. Ivashenko, P. Rudolf, B. J. van Wees, W. R. Browne, B. L. Feringa, *Chem. Eur. J.* **2011**, *17*, 8957 – 8964.
[36] M. Quintana, E. Vazquez, M. Prato, *Acc. Chem. Res.* **2013**, *46*, 138 – 148.
[37] D. N. Nguyen, H. Yoon, *Polymers* **2016**, *8*, 118.
[38] D.-W. Wang, F. Li, J. Zhao, W. Ren, Z.-G. Chen, J. Tan, Z.-S. Wu, I. Gentle, G. Q. Lu, H.-M. Cheng, *ACS Nano* **2009**, *3*, 1745 – 1752.
[39] Q. Wu, Y. Xu, Z. Yao, A. Liu, G. Shi, *ACS Nano* **2010**, *4*, 1963 – 1970.
[40] J. Xu, K. Wang, S.-Z. Zu, B.-H. Han, Z. Wei, *ACS Nano* **2010**, *4*, 5019 – 5026.
[41] J. Zhang, J. Jiang, H. Li, X. S. Zhao, *Energy Environ. Sci.* **2011**, *4*, 4009 – 4015.
[42] L. Lai, H. Yang, L. Wang, B. K. Teh, J. Zhong, H. Chou, L. Chen, W. Chen, Z. Shen, R. S. Ruoff, J. Lin, *ACS Nano* **2012**, *6*, 5941 – 5951.
[43] M. Xue, F. Li, J. Zhu, H. Song, M. Zhang, T. Cao, *Adv. Funct. Mater.* **2012**, *22*, 1284 – 1290.
[44] Y. Meng, K. Wang, Y. Zhang, Z. Wei, *Adv. Mater.* **2013**, *25*, 6985 – 6990.
[45] L. Li, X. Zhang, J. Qiu, B. L. Weeks, S. Wang, *Nano Energy* **2013**, *2*, 628 – 635.
[46] Y. Xu, M. G. Schwab, A. J. Strudwick, I. Hennig, X. Feng, Z. Wu, K. Müllen, *Adv. Energy Mater.* **2013**, *3*, 1035 – 1040.
[47] S. Giri, D. Ghosh, C. K. Das, *Adv. Funct. Mater.* **2014**, *24*, 1312 – 1324.
[48] L. Liu, Z. Niu, L. Zhang, W. Zhou, X. Chen, S. Xie, *Adv. Mater.* **2014**, *26*, 4855 – 4862.
[49] H. Sun, S. Xie, Y. Li, Y. Jiang, X. Sun, B. Wang, H. Peng, *Adv. Mater.* **2016**, *28*, 8431 – 8438.
[50] J. Wu, Q. E. Zhang, A. A. Zhou, Z. Huang, H. Bai, L. Li, *Adv. Mater.* **2016**, *28*, 10211 – 10216.
[51] H. Fan, N. Zhao, H. Wang, J. Xu, F. Pan, *J. Mater. Chem. A* **2014**, *2*, 12340 – 12347.
[52] P. Sekar, B. Anothumakkool, S. Kurungot, *ACS Appl. Mater. Interfaces* **2015**, *7*, 7661 – 7669.
[53] Y. Xu, Y. Tao, X. Zheng, H. Ma, J. Luo, F. Kang, Q.-H. Yang, *Adv. Mater.* **2015**, *27*, 8082 – 8087.
[54] X. Liu, Y. Zheng, X. Wang, *Chem. Eur. J.* **2015**, *21*, 10408 – 10415.
[55] Y. Liu, Y. Ma, S. Guang, H. Xu, X. Su, *J. Mater. Chem. A* **2014**, *2*, 813 – 823.
[56] Q. Liu, O. Nayfeh, M. H. Nayfeh, S.-T. Yau, *Nano Energy* **2013**, *2*, 133 – 137.
[57] K. Chi, Z. Zhang, J. Xi, Y. Huang, F. Xiao, S. Wang, Y. Liu, *ACS Appl. Mater. Interfaces* **2014**, *6*, 16312 – 16319.
[58] H. Choi, K.-J. Ahn, Y. Lee, S. Noh, H. Yoon, *Adv. Mater. Interfaces* **2015**, *2*, 1500117.
[59] S. Zhou, H. Zhang, Q. Zhao, X. Wang, J. Li, F. Wang, *Carbon* **2013**, *52*, 440 – 450.
[60] P. Yu, Y. Li, X. Zhao, L. Wu, Q. Zhang, *Langmuir* **2014**, *30*, 5306 – 5313.
[61] M. Liu, Y.-E. Miao, C. Zhang, W. W. Tjiu, Z. Yang, H. Peng, T. Liu, *Nanoscale* **2013**, *5*, 7312 – 7320.
[62] D. Li, Y. Li, Y. Feng, W. Hu, W. Feng, *J. Mater. Chem. A* **2015**, *3*, 2135 – 2143.
[63] J. Shen, C. Yang, X. Li, G. Wang, *ACS Appl. Mater. Interfaces* **2013**, *5*, 8467 – 8476.
[64] M. Mahmoud, F. E.-K. Maher, W. Hao, M. Andrew, Z. Qinqin, X. Jian, M. Peter, M. Jun, *Nanotechnology* **2015**, *26*, 075702.

[65] L. Li, A.-R. O. Raji, H. Fei, Y. Yang, E. L. G. Samuel, J. M. Tour, *ACS Appl. Mater. Interfaces* **2013**, *5*, 6622 – 6627.
[66] J. An, J. Liu, Y. Zhou, H. Zhao, Y. Ma, M. Li, M. Yu, S. Li, *J. Phys. Chem. C* **2012**, *116*, 19699 – 19708.
[67] G. Ning, T. Li, J. Yan, C. Xu, T. Wei, Z. Fan, *Carbon* **2013**, *54*, 241 – 248.
[68] N. Hu, L. Zhang, C. Yang, J. Zhao, Z. Yang, H. Wei, H. Liao, Z. Feng, A. Fisher, Y. Zhang, Z. J. Xu, *Sci. Rep.* **2016**, *6*, 19777.
[69] H.-P. Cong, X.-C. Ren, P. Wang, S.-H. Yu, *Energy Environ. Sci.* **2013**, *6*, 1185 – 1191.
[70] M. Kim, C. Lee, J. Jang, *Adv. Funct. Mater.* **2014**, *24*, 2489 – 2499.
[71] L. Lai, L. Wang, H. Yang, N. G. Sahoo, Q. X. Tam, J. Liu, C. K. Poh, S. H. Lim, Z. Shen, J. Lin, *Nano Energy* **2012**, *1*, 723 – 731.
[72] Y. Zhao, J. Liu, Y. Hu, H. Cheng, C. Hu, C. Jiang, L. Jiang, A. Cao, L. Qu, *Adv. Mater.* **2013**, *25*, 591 – 595.
[73] H. Kashani, L. Chen, Y. Ito, J. Han, A. Hirata, M. Chen, *Nano Energy* **2016**, *19*, 391 – 400.
[74] C. Zhu, J. Zhai, D. Wen, S. Dong, *J. Mater. Chem.* **2012**, *22*, 6300 – 6306.
[75] A. Davies, P. Audette, B. Farrow, F. Hassan, Z. Chen, J.-Y. Choi, A. Yu, *J. Phys. Chem. C* **2011**, *115*, 17612 – 17620.
[76] J. Zhang, P. Chen, B. H. L. Oh, M. B. Chan-Park, *Nanoscale* **2013**, *5*, 9860 – 9866.
[77] J. Zhu, Y. Xu, J. Wang, J. Wang, Y. Bai, X. Du, *Phys. Chem. Chem. Phys.* **2015**, *17*, 19885 – 19894.
[78] Z. Wang, P. Tammela, M. Stromme, L. Nyholm, *Nanoscale* **2015**, *7*, 3418 – 3423.
[79] J. Xu, D. Wang, Y. Yuan, W. Wei, L. Duan, L. Wang, H. Bao, W. Xu, *Org. Electron.* **2015**, *24*, 153 – 159.
[80] C. Bora, J. Sharma, S. Dolui, *J. Phys. Chem. C* **2014**, *118*, 29688 – 29694.
[81] S. Wang, L. Gai, H. Jiang, Z. Guo, N. Bai, J. Zhou, *J. Mater. Chem. A* **2015**, *3*, 21257 – 21268.
[82] J. Cao, Y. Wang, J. Chen, X. Li, F. C. Walsh, J.-H. Ouyang, D. Jia, Y. Zhou, *J. Mater. Chem. A* **2015**, *3*, 14445 – 14457.
[83] X. Yang, A. Liu, Y. Zhao, H. Lu, Y. Zhang, W. Wei, Y. Li, S. Liu, *ACS Appl. Mater. Interfaces* **2015**, *7*, 23731 – 23740.
[84] Y. Liu, J. Zhou, J. Tang, W. Tang, *Chem. Mater.* **2015**, *27*, 7034 – 7041.
[85] S. Wang, N. Liu, J. Su, L. Li, F. Long, Z. Zou, X. Jiang, Y. Gao, *ACS Nano* **2017**, *11*, 2066 – 2074.
[86] K. Sun, S. Zhang, P. Li, Y. Xia, X. Zhang, D. Du, F. H. Isikgor, J. Ouyang, *J. Mater. Sci. Mater. Electron.* **2015**, *26*, 4438 – 4462.
[87] Z.-S. Wu, Z. Liu, K. Parvez, X. Feng, K. Müllen, *Adv. Mater.* **2015**, *27*, 3669 – 3675.
[88] G. Qu, J. Cheng, X. Li, D. Yuan, P. Chen, X. Chen, B. Wang, H. Peng, *Adv. Mater.* **2016**, *28*, 3646 – 3652.
[89] S. Cho, M. Kim, J. Jang, *ACS Appl. Mater. Interfaces* **2015**, *7*, 10213 – 10227.
[90] K. Jo, M. Gu, B.-S. Kim, *Chem. Mater.* **2015**, *27*, 7982 – 7989.
[91] G. Yu, L. Hu, N. Liu, H. Wang, M. Vosgueritchian, Y. Yang, Y. Cui, Z. Bao, *Nano Lett.* **2011**, *11*, 4438 – 4442.
[92] X. Y. Zhang, A. Ciesielski, F. Richard, P. Chen, E. A. Prasetyanto, L. De Cola, P. Samori, *Small* **2016**, *12*, 1044 – 1052.
[93] L. Mao, Y. Li, C. Chi, H. S. On Chan, J. Wu, *Nano Energy* **2014**, *6*, 119 – 128.
[94] Z. Weng, Y. Su, D.-W. Wang, F. Li, J. Du, H.-M. Cheng, *Adv. Energy Mater.* **2011**, *1*, 917 – 922.
[95] H. Heli, H. Yadegari, A. Jabbari, *Mater. Chem. Phys.* **2012**, *134*, 21 – 25.
[96] X. Xia, D. Chao, Z. Fan, C. Guan, X. Cao, H. Zhang, H. J. Fan, *Nano Lett.* **2014**, *14*, 1651 – 1658.
[97] N. Q. Tran, B. K. Kang, S. N. Tiruneh, D. H. Yoon, *Chem. Eur. J.* **2016**, *22*, 1652 – 1657.
[98] P. A. Basnayaka, M. K. Ram, L. Stefanakos, A. Kumar, *Mater. Chem. Phys.* **2013**, *141*, 263 – 271.
[99] J. W. Park, S. J. Park, O. S. Kwon, C. Lee, J. Jang, J. Jang, J. W. Park, S. J. Park, C. Lee, O. S. Kwon, *Chem. Mater.* **2014**, *26*, 2354 – 2360.
[100] H.-B. Zhao, J. Yang, T.-T. Lin, Q.-F. Lü, G. Chen, *Chem. Eur. J.* **2015**, *21*, 682 – 690.
[101] K. Yuan, P. Guo-Wang, T. Hu, L. Shi, R. Zeng, M. Forster, T. Pichler, Y. Chen, U. Scherf, *Chem. Mater.* **2015**, *27*, 7403 – 7411.
[102] W. Ouyang, J. Sun, J. Memon, C. Wang, J. Geng, Y. Huang, *Carbon* **2013**, *62*, 501 – 509.
[103] B. Song, J. I. Choi, Y. Zhu, Z. Geng, L. Zhang, Z. Lin, C.-c. Tuan, K.-s. Moon, C.-p. Wong, *Chem. Mater.* **2016**, *28*, 9110 – 9121.
[104] Jaidev, S. Ramaprabhu, *J. Mater. Chem.* **2012**, *22*, 18775 – 18783.
[105] Y. Gogotsi, P. Simon, *Science* **2011**, *334*, 917 – 918.
[106] V. Aravindan, M. Ulaganathan, S. Madhavi, *J. Mater. Chem. A* **2016**, *4*, 7538 – 7548.
[107] Y. Ma, H. Chang, M. Zhang, Y. Chen, *Adv. Mater.* **2015**, *27*, 5296 – 5308.
[108] X. Y. Zhang, P. Samorì, *Angew. Chem. Int. Ed.* **2016**, *55*, 15472 – 15474; *Angew. Chem.* **2016**, *128*, 15698 – 15700.
[109] A. C. Forse, C. Merlet, J. M. Griffin, C. P. Grey, *J. Am. Chem. Soc.* **2016**, *138*, 5731 – 5744.
[110] Y. Shao, M. F. El-Kady, L. J. Wang, Q. Zhang, Y. Li, H. Wang, M. F. Mousavi, R. B. Kaner, *Chem. Soc. Rev.* **2015**, *44*, 3639 – 3665.

Manuscript received: March 9, 2017
Revised manuscript received: March 26, 2017
Accepted manuscript online: March 28, 2017
Version of record online: April 12, 2017